Journal of Hydroscience and Hydraulic Engineering
Vol. 23, No.1 May, 2005, 67-76

TWO-PHASE FLOW SIMULATION OF RAINFALL INFILTRATION AND SEEPAGE PROCESSES CONSIDERING HETEROGENEITY OF HYDRAULIC CONDUCTIVITY

BY

Masahiko Saito
Research Associate, Research Center for Urban Safety and Security,
Kobe University, Kobe, Japan

and

Takeshi Kawatani
Professor, Research Center for Urban Safety and Security,
Kobe University, Kobe, Japan

SYNOPSIS

To understand the effects of heterogeneity on rainfall infiltration and seepage, the governing equations of two-phase flow through porous medium are employed and the finite element formulation is carried out. The $1/f^{\zeta}$ model is introduced as a geostatistical model of hydraulic conductivity. Findings showed that when ground surface was under ponded condition, infiltrated water reached the groundwater table faster because of heterogeneity. However, when ground surface was under rainfall condition, the influence of heterogeneity depended on the size of domain analyzed. Moreover, the distribution of pore water pressure was strongly affected by spatial distribution of saturated hydraulic conductivity near the ground surface.

INTRODUCTION

It is important to understand rainfall infiltration process for slope stability or irrigations. Saturated-unsaturated seepage analysis (Neuman (4),(5)) has been commonly used for that purpose. However, previous studies report that the role of pore air flow cannot be ignored in rainfall infiltration process (Sato (8), Takagi & Morishita (9), Saito and Kawatani (7)). Moreover, in reality, the hydraulic properties of flow domain such as hydraulic conductivity are so heterogeneous that their aspects of whole flow domains are hardly described.

In this study, the governing equations of two-phase flow through porous medium are employed and the finite element formulation is carried out in order to ascertain the influence of pore air flow on rainfall infiltration and seepage. The $1/f^{\zeta}$ model is introduced as a geostatistical model of hydraulic

conductivity.

NUMERICAL SIMULATION

Governing Equations

The following equations for two-phase flow of air and water through porous medium (Meiri (1)) are used for generating the finite element model.

$$\phi \frac{dS_w}{dp_c}\left(\frac{\partial p_a}{\partial t}-\frac{\partial p_w}{\partial t}\right)=\frac{\partial}{\partial x_i}\left\{k_{rw}K_{ws}\left(\frac{\partial p_w}{\partial x_j}+\frac{\partial x_3}{\partial x_j}\right)\right\} \tag{1}$$

$$\phi\left\{(1-S_w)\frac{d}{dp_a}\left(\frac{1}{\beta_a}\right)-\frac{1}{\beta_a}\frac{dS_w}{dp_c}\right\}\frac{\partial p_a}{\partial t}+\frac{\phi}{\beta_a}\frac{dS_w}{dp_c}\frac{\partial p_w}{\partial t}=\frac{\partial}{\partial x_i}\left(\frac{k_{ra}}{\beta_a}K_{as}\frac{\partial p_a}{\partial x_j}\right) \tag{2}$$

where K_{ws} = the hydraulic conductivity at saturation; K_{as} = the air permeability; k_{rw}, k_{ra} = the relative permeabilities of water and air, respectively; p_a, p_w = the pressure heads of air and water, respectively; p_c = the capillary pressure; S_w = the saturation of water; ϕ = the porosity; β_a = the formation volume factor of air; t = the time; and x_i = the Cartesian coordinates (x_3 being the vertical coordinate oriented positive upward). The boundary conditions are described as the prescribed pressure and/or the prescribed flux.

Soil Water Retention Curve

The expressions proposed by van Genuchten (11) are used to describe the relationships between the capillary pressure, the degree of saturation and the relative permeabilities to the two fluids.

$$S_e=\frac{S_w-S_r}{1-S_r}=\left\{1+(\alpha p_c)^n\right\}^{-m} \tag{3}$$

$$k_{rw}=S_e^{\varepsilon}\left\{1-\left(1-S_e^{1/m}\right)^m\right\}^2 \tag{4}$$

$$k_{ra}=(1-S_e)^{\gamma}\left(1-S_e^{1/m}\right)^{2m} \tag{5}$$

where S_e = the effective saturation; S_r = the residual saturation; α, n, m = parameters; ε, γ=parameters which describe the connectivity of pores (Mualem(2)). dS_W/dp_C is given by Eq.6.

$$\frac{dS_w}{dp_c} = -\alpha mn(1-S_r)(\alpha p_c)^{n-1}\left\{1+(\alpha p_c)^n\right\}^{-m-1} \tag{6}$$

Viscosity of Air and Water

The viscosity of water is the function of temperature given by Eq.7.

$$\mu_w(t_w) = \frac{\mu_{w0}}{1+3.368\times10^{-2}t_w+2.2099\times10^{-4}t_w{}^2} \tag{7}$$

where t_w= the temperature of water in centigrade; μ_{WO} = the viscosity of water at t_W=0 ℃ and 1 atm(=1.78×10^{-3} Pa・s).

The viscosity of air is the function of the absolute temperature given by Eq.8.

$$\mu_a(T_a) = \mu_{a0}\left(\frac{T_a}{T_{a0}}\right)^{2/3} \tag{8}$$

where μ_{a0} = the viscosity of air at T_a=273.2 (K) and 1 atm(=1.72×10^{-5} Pa・s); T_a =the absolute temperature of air; T_{a0} =273.2 (K). Pressure dependency of viscosity for air and water is ignored.

Geostatistical Model of Hydraulic Conductivity

The covariance function or the semi-variogram is often used to approximate the geostatistical aspect of spatial distribution of hydraulic conductivity though its theoretical background is not clear. On the other hand, Saito and Kawatani (6) proposed the $1/f^{\zeta}$ model based on stochastic fractal approach, and they verified that the model could simulate the statistical characteristics of natural flow field such as the scale dependency of the integral scale.

In this model, the spectral density of the hydraulic conductivity in the logarithmic scale, $Y(x,y)=\log(K_W(x,y))$, is defined as

$$S_Y(|f|) \propto |f|^{-D} \tag{9}$$

where S_Y = the spectral density; f = the wavenumber vector; D = the space dimension.

The variance of Y is proportional to the logarithmic value of the resolution.

$$\sigma^2 = \lambda \log_{10} N \tag{10}$$

where σ^2 = the variance of Y; λ = the constant; N = the resolution.

Spatial Distribution of van Genuchten Parameters

According to laboratory-test results reported by Taninaka and Ishida (10) and Nakagawa et al. (3)(Figure 1), the relationship between K_{WS} and the parameter $1/\alpha$ can be expressed as follows:

$$1/\alpha = -37.35 \times \log_{10} K_{ws} - 16.22 \qquad (11)$$

where α = the van Genuchten parameter(1/cm); K_{WS} = the hydraulic conductivity at saturation(cm/s). The other parameters (n and S_r) are assumed to remain constant.

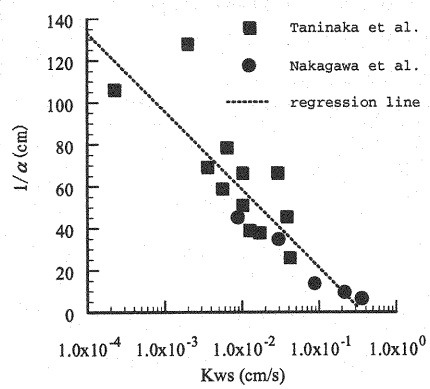

Fig. 1 The relationship between K_{ws} and the parameter $1/\alpha$

Simulation Model

Figure 2 depicts the flow domain for this study. The conditions for simulation are listed in Table 1. The simulations are performed in cases of both a ponded condition and a rainfall condition. In each case, a comparison is made between the results for uniform field and non-uniform field. Figure 3 shows an example of the distributions of the logarithmic value of hydraulic conductivity K_{WS}. The average value of K_{WS} is 10^{-4} cm/s.

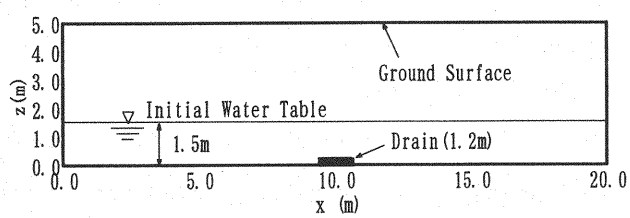

Fig. 2 Flow domain of simulation

Table 1 Properties and conditions of analysis

	Uniform/Non-uniform	Ground surface	Domain size
Case-1A	Uniform	Ponded	20 m ×5 m
Case-1B	Non-Uniform	Ponded	20 m ×5 m
Case-2A	Uniform	Rainfall	20 m ×5 m
Case-2B	Non-uniform	Rainfall	20 m ×5 m
Case-3A	Uniform	Rainfall	40 m ×10 m
Case-3B	Non-uniform	Rainfall	40 m ×10 m

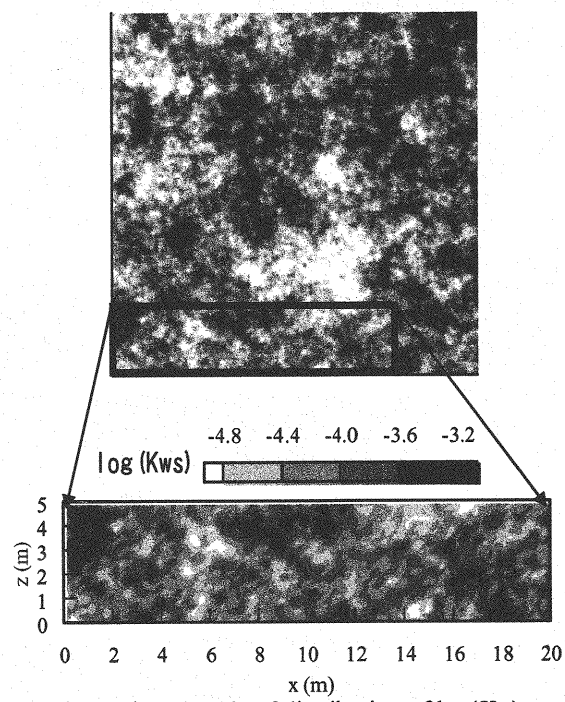

Fig. 3 The example of distribution of $\log(K_{ws})$

RESULTS AND DISCUSSION

Ponded Condition

Two cases are simulated for the ponded conditions (Case-1A: uniform field, Case-1B: non-uniform field). The pressure heads of air and water on the ground surface are 0(m). In Case-1B, 100 Monte Carlo runs are carried out. Figure 4 shows the ensemble mean of discharge from drain (=Q) in Case-1A and Case-1B. The increase of discharge begins earlier in the non-uniform field than in the uniform field, because water infiltrated from ground surface reaches groundwater table earlier in the former case. On the other hand, there is no difference in the discharge between these two cases at t=6 days. Figure 5 shows an example of the distributions of both saturation and velocity of water at t=3 days. In Case-1B, the spatial variation of velocity is very large and a greater velocity is observed

in the central zone. A comparison made between these two cases indicates that when the model is assumed to be a uniform field such as Case-1A, the time for the infiltrated water to reach groundwater table could be overestimated.

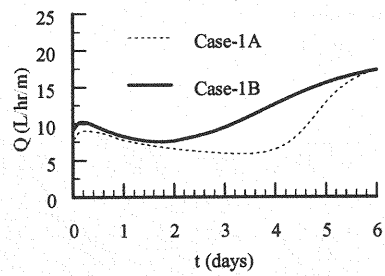

Fig. 4 Discharge from drain

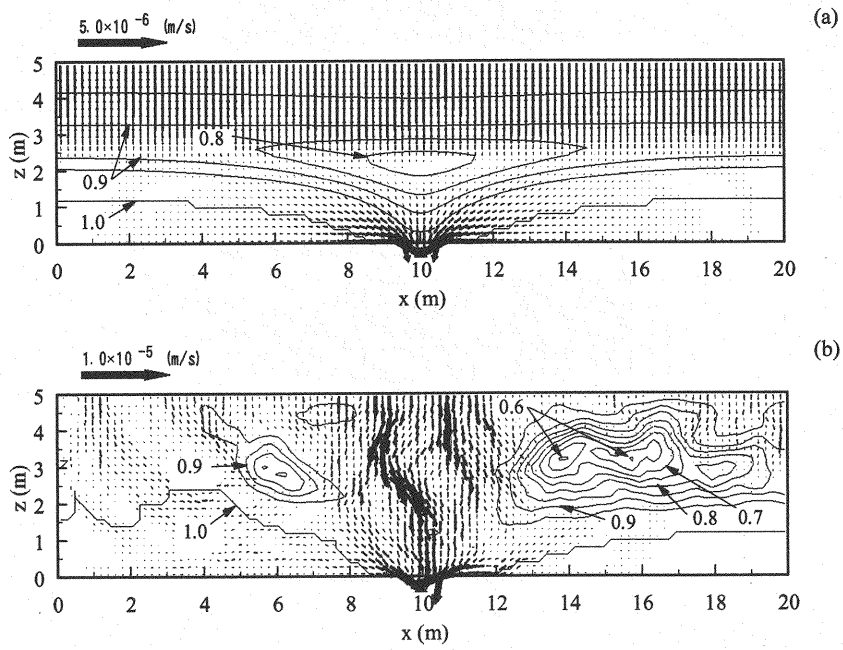

Fig. 5 Distribution of degree of saturation and velocity of water at t=3.0 days.
(a) Case-1A, (b) Case-1B

Rainfall Condition

Four cases (i.e., Case-2A, Case-2B, Case-3A and Case-3B listed in Table 1) are simulated for the rainfall conditions. Figure 6 shows the rainfall condition employed for the simulations. In Case-2B and Case-3B, 100 Monte Carlo runs are carried out. Figure 7 shows an ensemble mean of the discharge from drain. The results suggest that the influence of heterogeneity depends on the domain size. Figure 8 shows the distribution of the unsaturated hydraulic conductivity in a logarithmic scale.

The variation of hydraulic conductivity in the horizontal direction is less in Case-3B than in Case-2B. In the large domain, since the infiltration process is governed by the unsaturated hydraulic conductivity whose variation is quite small in general, the effect of heterogeneity appears to decrease.

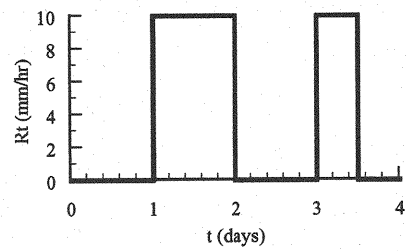

Fig. 6 Rainfall condition

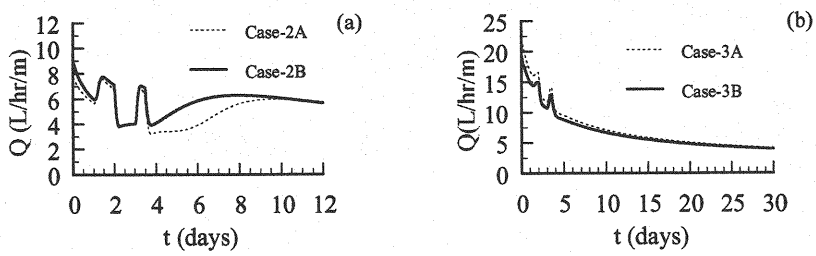

Fig. 7 Discharge from drain (a) Case-2A, 2B, (b) Case-3A, 3B

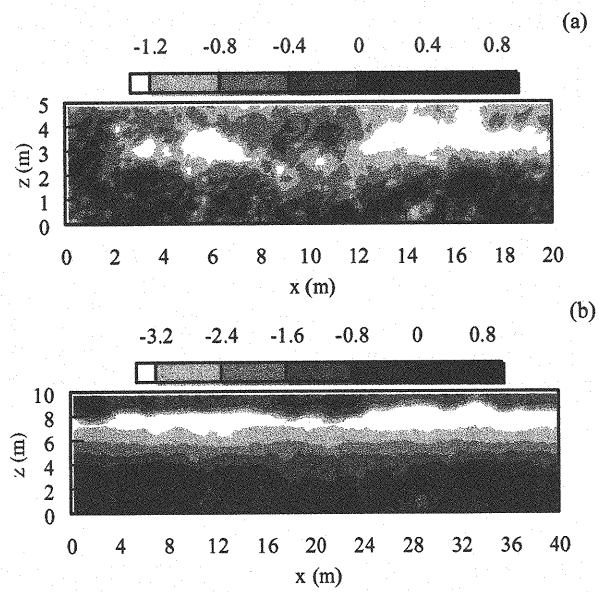

Fig. 8 Distribution of log unsaturated hydraulic conductivity (a) Case-2B, (b) Case-3B

Influence of Heterogeneity on Pore Pressure Distribution

It is generally thought that discharge from drain reflects the average properties of the domain while the pore pressure distribution directly reflects the distributions of hydraulic properties. Furthermore, the influence of heterogeneity on pore water pressure distribution is investigated in the domain shown in Figure 3. Figure 10 depicts the change of pore water pressure with time in Case-2 and Case-3 at the points shown in Figure 9. Figure 11 shows an example of the distributions of water pressure head at t=6 days.

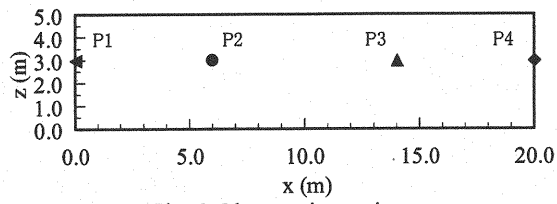

Fig. 9 Observation points

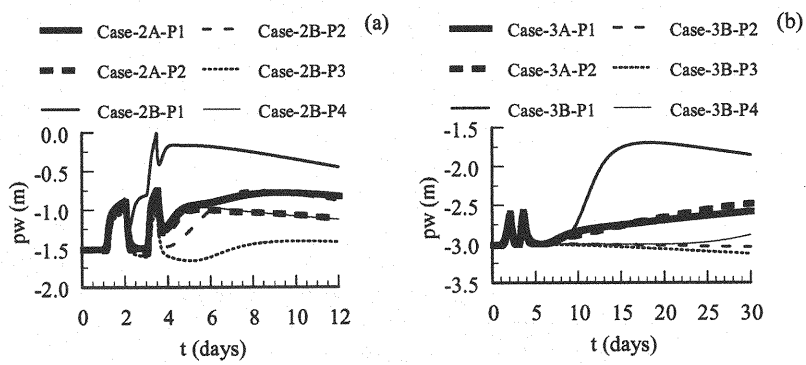

Fig. 10 Change of pore pressure (a) Case-2, (b) Case-3

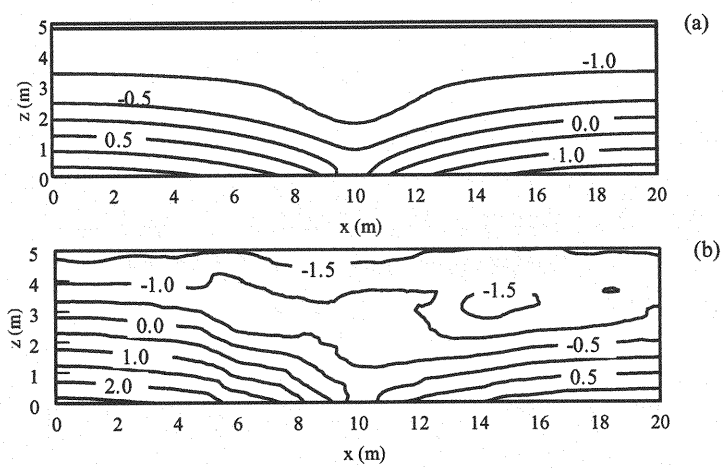

Fig. 11 Distribution of pressure head at t=6 days (a) Case-2A, (b) Case-2B

Findings reveal that the distribution of pore water pressure is non-symmetric even though there is no difference between the mean values of $Y=(\log(K_{ws}))$ in the left zone and the right zone as far as the whole flow field is concerned. This non-symmetrical distribution is due to the fact that the mean value of the saturated hydraulic conductivity near the ground surface is larger in the left zone than in the right zone.

These results indicate that the distribution of pore water pressure strongly depends on the distribution of hydraulic conductivity near ground surface.

CONCLUSIONS

Findings of this study can be summarized in the following statements:

1. When ground surface was under the ponded condition, surface water reached the water table faster because of heterogeneity.
2. When ground surface was in non-ponded condition, the influence of heterogeneity depended on analysis scale.
3. Distribution of pore water pressure was closely related to distribution of saturated hydraulic conductivity of ground surface.

REFERENCES

1. Meiri, D. : Two-phase flow simulation of air storage in an aquifer, Water Resources Research, Vol.17, No.5, pp.1360-1366, 1981.
2. Mualem, Y.:A new model for predicting the hydraulic conductivity of unsaturated porous media, Water Resources Research, Vol.12, pp.513-522, 1976.
3. Nakagawa, K., Iwata, M., Chikushi, J. and Momii, K. :Unsaturated water flow and solute transport in artificially distributed hydraulic conductivity field, Journal of hydro science and hydraulic engineering, Vol.21, No.2, pp.37-45,2003.
4. Neuman, S. P. : Saturated unsaturated seepage by finite elements, Proc., ASCE HY, Vol.99, No.12, pp.2233-2250, 1973.
5. Neuman, S.P. : Galerkin method of analyzing non-steady flow in saturated-unsaturated porous media, Finite Element Method in Flow Problem, edited by C. Taylor, O.C. Zienkiewicz, R.H. Gallagher, John Wiley & Sons, Chap.19,1974.
6. Saito, M. and Kawatani, T. : Theoretical study on spatial distribution of hydraulic conductivity, Journal of Geotechnical Engineering, Vol.645, III-50, pp.103-114, 2000(in Japanese with English abstract).
7. Saito, M. and Kawatani, T. : Numerical study on rainfall infiltration and seepage processes

considering pore-air flow, Journal of Applied Mechanics, JSCE, Vol.6, pp.865-872, 2003(in Japanese with English abstract).

8. Sato, K. : A theoretical consideration on vertical infiltration affected by compressed air pressure of voids in soil, Proceedings of JSCE, Vol.216, pp.21-28, 1973(in Japanese with English abstract).
9. Takagi, F. and Morishita, T. : Analysis of vertical infiltration as two-phase flow, Proceedings of JSCE, Vol.271, pp.37-44, 1978(in Japanese with English abstract).
10. Taninaka, H. and Ishida, T. : An examination of relative permeability curve (θ-k, relationship) of sandy soil, Proceedings of the Thirty-Third Japan National Conference on Geotechnical Engineering, Vol.2, pp.1817-1818, 1998(in Japanese).
11. van Genuchten, M. T. : A closed-form equation for predicting the hydraulic conductivity of unsaturated soils, Soil Science Society American Journal, Vol.44, pp.892-898, 1980.

(Received July 2, 2004; revised October 15, 2004)